Iranian Journal of Science & Technology, Transaction A, Vol. 33, No. A4
Printed in the Islamic Republic of Iran, 2009

SELECTIVE NANOSENSING OF COPPER (II) ION USING L-LYSINE FUNCTIONALIZED GOLD CYSTEAMINE SELF-ASSEMBLED MONOLAYER*

R. SHABANI[1], S. A. MOZAFFARI[2], S. W. HUSAIN[1] AND M. SABER TEHRANI[1**]

[1]Department of Chemistry, Islamic Azad University, Science and Research Branch, P.O. Box: 145-775, Tehran, I. R. of Iran, m.sabertehrani@yahoo.com
[2]Advanced Institute of Technology, Iranian Research Organization for Science and Technology (IROST), P.O. Box: 15815-3538, Tehran, I. R. of Iran

Abstract – Fabrication of a cysteamine (CA) self-assembled monolayer (SAM) modified gold electrode *in-situ* functionalized with L-Lysine (Lys) is presented and described. The fabricated electrode was used for highly selective and sensitive accumulation and the determination of copper ions (Cu^{2+}) in a nanomolar concentration. Techniques like cyclic voltammetry (CV) and electrochemical impedance spectroscopy (EIS) with an external redox probe (p-Benzoquinone) were used to investigate the layer-by-layer self assembly modification on a gold electrode, monolayer structure and the ion permeation through it. The differential pulse voltammetric (DPV) method was used for determination of Cu^{2+}. The results indicated that DPV peaks currents have a linear relationship with pCu in the concentration range of 1.0×10^{-12} - 1×10^{-6} M, with a correlation coefficient of 0.9982. The detection limit could be estimated 1.2×10^{-13} M according to the IUPAC recommendation (3σ).

Keywords – Self-assembled monolayer, L-Lysine, Electrochemical impedance spectroscopy, Copper (II) ion

1. INTRODUCTION

Self assembled monolayers (SAMs) have been described as a spontaneous, coordinated chemical interaction of individual molecular building blocks to create a stable, highly ordered and densely packed single layer of molecules from a solution or a gas phase onto a substrate [1-3]. Over the past two decades, SAMs have received extensive attention due to their stability, simple formation and potentiality of application in many fields such as sensor and biosensor construction [4, 5], studies of charge transfer kinetics [6], resistance to corrosion [7], molecular electronics [8, 9], biomolecular electronic devices [10], immobilization of biocatalyst [11, 12], drug delivery [13], and trace ion determination [14-18].

Electrode modification through the self-assembly process profits from chemical specificity, rapid response, high sensitivity, antifouling effect, and possibility for *in-situ* immobilization of biological recognition agents (e.g., enzymes) [19-25]. Although it is possible to have a wide range of organic functionalities on the surface of the electrode with the desired properties of SAM's tail groups, one of the limitations of this research area involves the synthesis and testing of macrocyclic ligands with selectivity and sensitivity for a target metal ion. The common strategies for overcoming this limitation and introducing selective functionalities into the electrode surface via thiol SAMs are: (*i*) *Ex-situ* functionalization of thiols, adsorption of the single component and then filling the defects with shorter monolayers (preparing mixed SAMs on the surface) [26]. A number of drawbacks are inherent in this method [4, 27]. (*ii*) Changing the surface group's homogeneity or heterogeneity, surface charges position

*Received by the editor August 30, 2010 and in final revised form December 28, 2010
**Corresponding author

and strength using mixed self-assembled monolayers which are affected by internal interactions between the monolayers [28]. (*iii*) *In-situ* functionalization by using a simple SAM (e.g. cysteamine) as a platform to immobilize biological species for biosensor applications or to anchor desired chemical functions to the surface [4, 29]. Modification of the exposed surface of a SAM after formation offers some advantages which are described elsewhere [2].

Exploiting the molecular level control over the fabrication of a sensing interface afforded by SAMs for metal ions was first demonstrated by Rubinsten *et al.*, where a modified gold electrode with mixed SAMs which detect a low level of Cu^{2+} ions (10^{-7} M) with minimal interference from Fe^{2+} ions, was introduced [30-32]. Until now, a variety of monolayers (as a single layer) have been used for metal ion analysis [14, 18, 33-36], and the results have shown that the achievement to high selective and sensitive metal ions recognition is limited. However, a high degree of selectivity in nature for the binding of copper ions is achieved using amino acids and peptide motifs. As a consequence of the selectivity of amino acids and peptide motifs for some metal ions, there is a growing interest in exploiting this selectivity for analytical purposes [37]. Gooding and co-workers found a different approach by employing a covalently attached tripeptide Gly–Gly–His to a 3-mercaptopropionic acid (MPA) modified gold electrode and reported a detection limit lower than 3 pM for Cu^{2+} [38]. They also developed the use of peptides for detecting metals electrochemically. They explained that the peptide modified electrodes exhibit high sensitivity to copper, which is attributed to the stable 4N coordinate complex the peptide formed around the metal ion to give copper the preferred tetragonal coordination [39, 40].

In this study, taking advantage of the copper ion binding by amino acids and peptides, and designing electrodes with controllable surface properties of amino acids using the in-situ functionalization method, we report a new approach for sensitive and selective copper ion detection by an L-Lysine functionalized self-assembled monolayer on gold surface.

2. EXPERIMENTAL

a) Materials and Reagents

Analytical grade of cysteamine ($HSCH_2CH_2NH_2.HCl$), CA; glutaraldehyde ($C_5H_8O_2$, 25% v/v, in water), GA; L-Lysine ($NH_2(CH_2)_4CH(NH_2)COOH$), Lys; *p*-benzoquinone as redox probe; and ethylendiaminetetraacetic acid (EDTA) were obtained from Merck, and used as received. All solutions were prepared with deionized water. Phosphate buffer solutions (PBS) were prepared using Smally's method [41].

b) Apparatus

The cyclic voltammetry (CV), electrochemical impedance spectroscopy (EIS), and differential pulse voltammetry (DPV) measurements were performed using Autolab® 30 Potentiostat/Galvanostat equipped with a Frequency Response Analyzer, interfaced with a PCIII 800MHz, and controlled by GPES and FRA 4.9 softwares (Eco Chemie, Utrecht, The Netherlands). The electrochemical measurements were performed in a conventional three-electrode glass cell including a gold disk (0.0314 cm^2, Metrohm) SAM modified electrode as the working, a large surface area Pt plate (99.99%, 5 cm^2) as auxiliary, and an Ag/AgCl electrode as the reference electrode. All reported potentials are referenced to the saturated Ag/AgCl electrode. The measurements were carried out at room temperature. The cell purged with N_2 at all electrochemical measurements.

The EIS measurements were performed in the presence of a 5 mM PBQ as the redox probe. A 5 mV AC amplitude potential superimposed on the formal potential of the redox probe ($E^{0'}$ = -0.05 for PBQ) was applied and a wide range of frequencies from 10 kHz to 10 mHz at five discrete frequencies per decade

was scanned. The impedance spectra were plotted in the form of complex plane diagrams (Nyquist plots). The EIS data analysis was performed using the ZView® version 2.3f software and CNLS approximation method. CPE model was used to explain the whole frequency range of data from which analytical information was extracted [42].

c) Electrode Modification

Before chemical modification, the gold electrode surface was cleaned first physically by polishing with alumina slurries (Buehler®, starting from 0.3 down to 0.05 μm), rinsing with ethanol and deionized water, and sonicating in water/chloroform/water respectively, for 5 min, to remove all physically adsorbed species; then electrochemically by cycling the electrode potential between 0.0 to +1.5 V *vs.* Ag/AgCl in 0.5 M H_2SO_4 until a reproducible voltammogram was obtained. Finally, the electrodes were cleaned in freshly prepared "piranha" solution (Piranha solution is a 1:3 (v/v) mixture of 30% H_2O_2 and concentrated H_2SO_4. *Warning*: Piranha solution is extremely corrosive and must be handled carefully) for 3.0 min and rinsed thoroughly with double distilled water. A roughness factor 1.9± 0.15 was calculated from the ratio of the real to geometric surface area. The real surface area was estimated from integration of the cathodic peak observed during the redox reaction of gold in 0.5 M H_2SO_4, assuming a 482 μC cm^{-2} charge for the reduction of one monolayer of AuO on Au(111) [43], and we attempted to maintain it constant in all experiments. Preparation of the Au-CA-GA-Lys electrode was performed in a three step method: (*i*) immediately after cleaning, the bare gold (Au) was immersed into 18 mM CA aqueous solution for 4 hours at room temperature in darkness to form Au-CA, washed with purified water to eliminate physically adsorbed cysteamine, (*ii*) the Au-CA modified electrode was soaked in PBS (pH=7.0) containing 12% (v/v) GA solution for 1 h to form Au-CA-GA, and rinsed with water, (*iii*) the Au-CA-GA electrode was dipped into a 0.01 M L-Lysine ethanolic solution for 2 hours to form Au-CA-GA-Lys SAM by means of Schiff's base formation [4] between the aldehyde groups of GA and the amino groups of L-Lysine. Finally, the modified electrode (Au-CA-GA-Lys) was removed, washed with water and used for electrochemical measurements (Scheme 1). Pre-concentration of Cu^{2+} ions was carried out by dipping the Au-CA-GA-Lys SAM modified electrode into a 5 ml of stirred solution containing the supporting electrolyte, and the desired concentration of Cu^{2+} with a known pH, under open-circuit potential (OCP) for a set time to form Au-CA-GA-Lys-Cu^{2+}. The electrode was then removed and rinsed with a copper-free PBS and used immediately for electrochemical measurements.

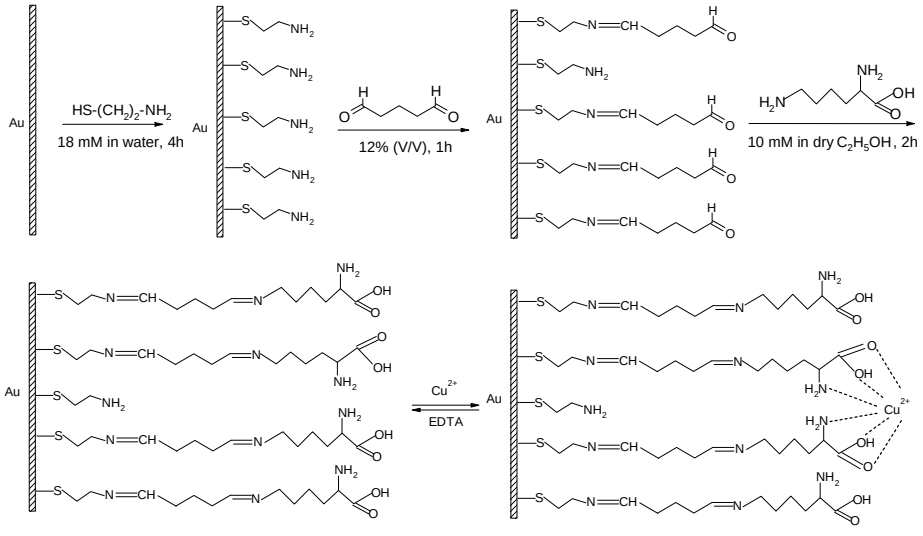

Scheme 1. Schematic illustration of proposed mechanism for self assembly process and Cu^{2+} ion interaction with the modified electrode

3. RESULTS AND DISCUSSION

a) Characterization of Au-CA-GA-Lys Electrode

Cyclic voltammetry: The stepwise assembly of the layered functionalized electrode was traced by cyclic voltammetry and electrochemical impedance spectroscopy. The electrochemical responses in each step were investigated to confirm the layer by layer assembly process. Figure 1 shows the voltammograms of the bare gold electrode, Au (curve a), modified electrode with cysteamine, Au-CA (curve b), activation with glutaraldehyde, Au-CA-GA (curve c), functionalization with L-Lysin, Au-CA-GA-Lys (curve d), and modified gold electrode after immersing in 1.0×10^{-4} M Cu^{2+} for 5 min, Au-CA-GA-Lys-Cu^{2+} (curve e) in copper-free PBS (pH 7.0). The voltammograms suggest that the layers are electrochemically inactive in the range of 0.6 to –0.2 V *vs.* Ag/AgCl.

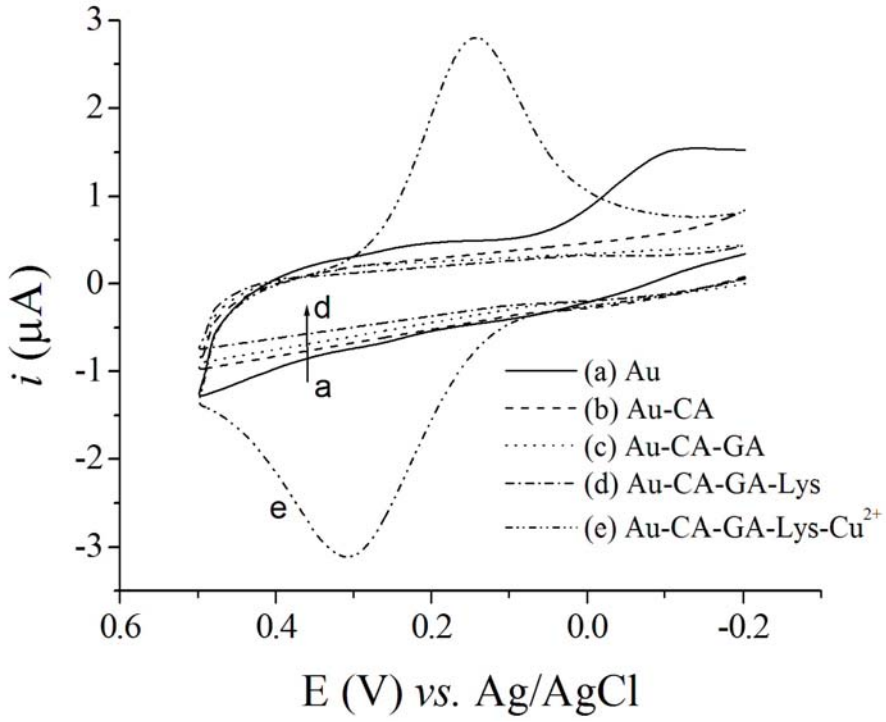

Fig. 1. Cyclic voltammograms were obtained on bare Au (a), Au-CA (b), Au-CA-GA (c), Au-CA-GA-Lys (d), and Au-CA-GA-Lys-Cu^{2+} (e) in copper free PBS (pH = 7.0), and 0.1 M $NaClO_4$; scan rate: 100 mV s^{-1}

Figure 2 shows the cyclic voltammograms of the layers mentioned in Scheme 1 in the presence of the PBQ redox probe. The reversible electrochemical behavior and large current density of the redox waves indicates that the redox couple can easily access the electrode surface of the bare Au electrode (Fig. 2 curve a). While, the addition of the cysteamine monolayer onto the electrode does not show any considerable effect in the peak potential separation (Fig. 2 curve b), the heterogeneous electron transfer from the gold electrode to the redox couple in aqueous solution was hardly influenced by the presence of the activation and functionalization of cysteamine monolayers (Fig. 2 curves c and d), and indicating that the redox couple still cannot easily access the electrode surface. With the addition of the CA monolayer onto the gold surface, the activation of CA with GA, and then the functionalization by Lys, it was observed that the peaks current decreases and irreversibility (ΔE_p) of the redox probe reaction increases as a result of the layer by layer assembly. The results show that further layer-by-layer assembly on the electrode was influenced by the addition in chain length, which retards the interfacial electron-transfer

kinetics of the redox probe, resulting in the perturbation of the reversible behavior of the redox probe. The results obtained for conditioning of the Au-CA-GA-Lys electrode in 1.0×10^{-4} M Cu^{2+} (Fig. 2 curve e) prove the tailoring effect of Cu^{2+} ions on the monolayer surface. A similar result was reported for the presence of uranyl ions on the surface of phosphate functionalized cysteamine SAMs modified gold electrode, which confirms the increase in charge transfer resistance caused by the tailoring effect of accumulated ions at the surface of the monolayer [16, 29].

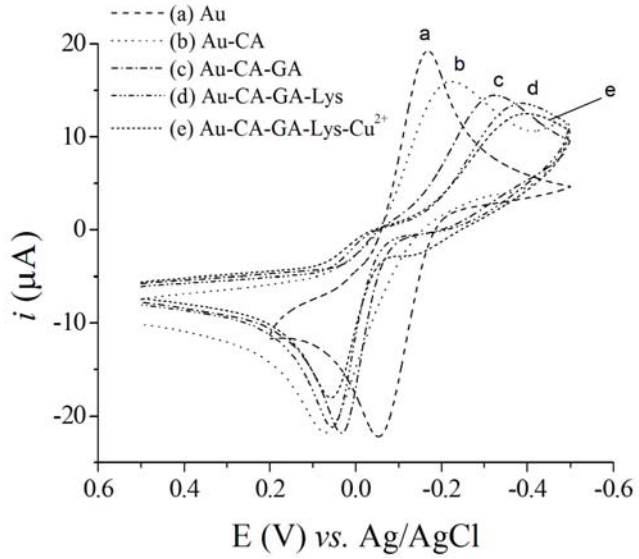

Fig. 2. Cyclic voltammograms were obtained on bare Au (a), Au-CA (b), Au-CA-GA (c), Au-CA-GA-Lys (d), and Au-CA-GA-Lys- Cu^{2+} (e) in 5 mM PBQ; scan rate: 100 mV s^{-1}

Impedance spectroscopy: Electrochemical methods are simple and low operating cost methods for the study of the interfacial event at modified electrodes. Among the electrochemical methods, EIS is a powerful, informative, and non-destructive method that can be used to study the interfacial events [44-46], and serve as a transducer to trace the *blocking behaviors* (as complexation / precipitation) [29], *electrostatic interactions* (by charged surfaces with charged probes) [28] and *diffusion behavior / electrocatalytic effects* at modified electrodes [4].

The EIS measurements were used to trace the events during the formation of Au-CA-GA-Lys electrode, and its interaction with the external probe after the Cu^{2+} accumulation. Figure 3 shows the Faradaic impedance spectra presented as Nyquist plots (Z'' *vs.* Z') upon the assembly of the layers on the electrode in the presence of the PBQ redox probe. The bare Au electrode exhibits an almost straight line (Fig. 3 curve a and inset) that is characteristic of a mass diffusional limiting electron–transfer process. Assembly of the cysteamine monolayer on the electrode surface generates a layer on the electrode that introduces a barrier to the interfacial electron-transfer. This is reflected by the appearance of the semicircle part on the spectrum (Fig. 3 curve b). The addition of GA on the cysteamine monolayers and then Schiff's base formation of Lys on the GA layer results in an increase of the electron-transfer resistance (Fig. 3 curve c, and d). The covalent attachment of each layer increases the charge transfer resistance. These results are consistent with the stepwise build up of the three layers on the electrode surface (see Scheme 1). However, conditioning of the functionalized electrode in 1.0×10^{-4} M Cu^{2+} (Fig. 3 Curve e) shows increase in the redox charge transfer resistance in the presence of PBQ probe which proves the tailoring effect of Cu^{2+} ions on the monolayer surface. The EIS data obtained on the modified Au-CA-GA-Lys electrode in different steps are well approximated by Constant Phase Element (CPE) model (Fig. 4) [47, 48].

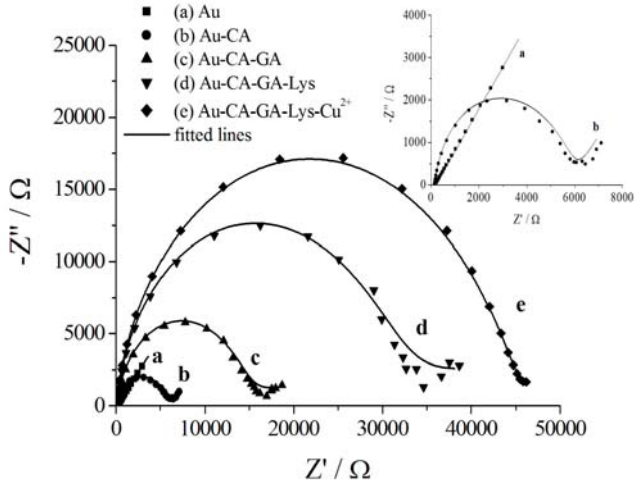

Fig. 3. Complex plane plots (Z" *vs.* Z′) obtained for the faradaic impedance measurements in the same conditions as Fig. 2. The inset shows curves a and b with a higher resolution scale. Symbols indicate experimental and solid lines approximated data.

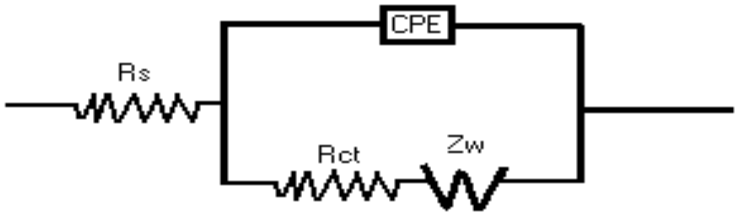

Fig. 4. Equivalent circuit (CPE model) used for impedance data approximation: R_s, R_{ct}, CPE, and Z_w represent the solution resistance, charge-transfer resistance, constant-phase element, and Warburg impedance, respectively

b) Optimization of the Experimental Conditions

Time: The modified electrode was immersed in a 5.0 $\times 10^{-5}$ M Cu^{2+} solution with pH=7.0 and then DPV was obtained in copper-free PBS with pH=5.0 for different periods of time. Figure 5 shows the response of the modified electrode *vs.* time. The maximum peak current was observed at 9 min.

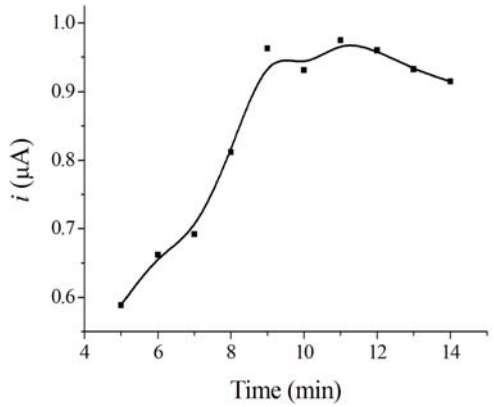

Fig. 5. Response of Au-CA-GA-Lys modified electrode as a function of accumulation time. Accumulation conditions: 5.0 $\times 10^{-5}$ M Cu^{2+} in PBS (pH=7.0) and 0.1 M $NaClO_4$, at the open-circuit potential. Measurement conditions: 0.1 M copper-free PBS (pH=5.0)

pH of the accumulation and determination solutions: The dependence of cathodic DPV current on the pH conditions for the accumulation and determination steps was investigated. The 5.0×10^{-5} M Cu^{2+} solutions with pH=3.0 to 8.0 were prepared using PBS. Then, the Au-CA-GA-Lys modified electrode was immersed in each solution for 9 min. The modified electrode was rinsed with buffer and then DPV was obtained in copper free PBS with pH=5.0. Figure 6 (curve a) shows the dependence of the current on the pH of the accumulation solution. This curve indicates the maximum accumulation of Cu^{2+} takes place at pH=6.5. At pH lower than 6.5 accumulation decreases due to H^+ competition with Cu^{2+} for functional groups of the modified electrode surface. In the pH values higher than 6.5, OH^- compete with surface functional groups for Cu^{2+}. To optimize pH conditions for the determination step, the cathodic current was obtained after accumulation of 5.0×10^{-5} M Cu^{2+} with pH=6.5 for 9 min in the PBS determining solutions at a pH range 3.0 to 8.0. Figure 6 (curve b) indicates that maximum current was obtained at pH=6.0. At pH values higher than 6.0, hindering the charge transfer kinetics between Cu^{2+} and the metallic electrode base may be related to: (*i*) speciation of Cu^{2+} or (*ii*) different strength of interactions between Cu^{2+} and functional groups of the modified electrode at different pHs. At pH lower than 6.0, some parts of the Cu^{2+} will leave the surface before starting the reduction step.

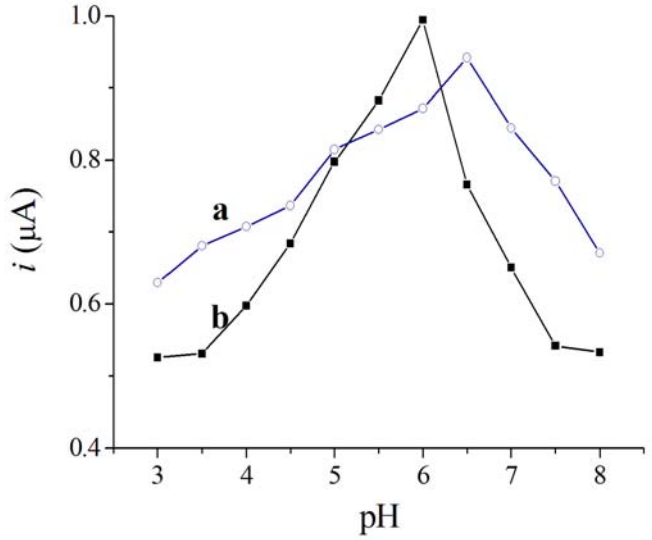

Fig. 6. Response of Au-CA-GA-Lys SAM-modified electrode as a function of pH: (a) accumulation step, and (b) determination step. Accumulation conditions: 5×10^{-5} M Cu^{2+}, time (9 min) at the open-circuit potential with determination at pH= 5.0. Determination conditions: 0.1 M $NaClO_4$, copper-free PBS with accumulation at pH= 6.5

c) Calibration Curve, Detection Limit and Repeatability

Under optimized conditions, the DPVs for pre-adsorbed Cu^{2+} by the Au-CA-GA-Lys electrode were obtained (Fig. 7). The DPV current around +200 mV in various concentrations of Cu^{2+} was recorded. Figure 7 (inset) shows that the DPV peak current is linear *vs.* pCu in the range of 1.0×10^{-12} - 5.0×10^{-6} M ($i_{(\mu A)}$=1.41718 (±0.01968) - 0.07946 (±0.00213)×pCu $_{(M)}$, r = 0.9982). The detection limit calculated from the signal equals 3σ (standard deviation) of the background noise and was 1.2×10^{-13} M Cu^{2+}. The repeatability of the method was obtained for n = 9 at 5.0×10^{-7} M Cu^{2+} with a relative standard deviation (RSD) of 4.1%. The stability of the sensor was studied by comparing the electroanalytical response of the electrode for a series of repeated determination. The relative changes in the sensor responses for more than 100 measurements were lower than 5%.

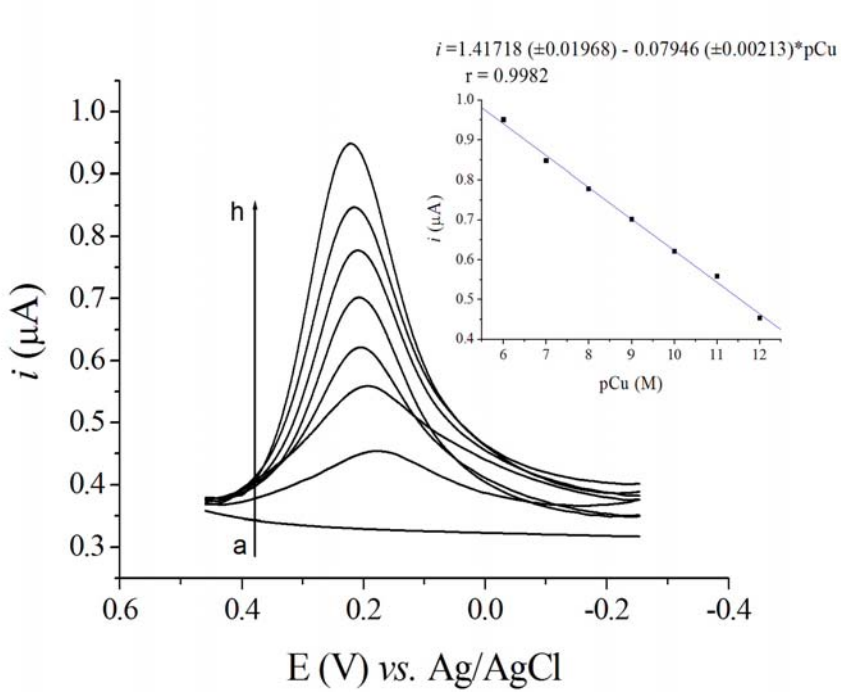

Fig. 7. Differential pulse voltammograms obtained on Au-CA-GA-Lys SAM modified electrode as a function of Cu^{2+} ion concentrations: (a) 0.0, (b) 1.0×10^{-12}, (c) 1.0×10^{-11}, (d) 1.0×10^{-10}, (e) 1.0×10^{-9}, (f) 1.0×10^{-8}, (g) 1.0×10^{-7}, and (h) 1.0×10^{-6} M in 0.1 M PBS (pH = 6.5), and 9 min accumulation time; the inset shows calibration curve. Stripping conditions: 0.1 M PBS (pH = 6.0); Optimized instrumental parameters: pulse amplitude 0.050 V, sweep rate 0.050 V s^{-1}, pulse time 0.040 s, and voltage step 0.010 V

d) Analytical Applications

The Au-CA-GA-Lys electrode was used to determine the Cu^{2+} content of two synthetic solutions (Table 1). The results clearly imply the potential application of the fabricated sensor for the analysis of a low level of Cu^{2+}.

Table 1. Results obtained for Determination of Cu^{2+} in synthetic solutions using modified electrode

sample	found	% recovery
synthetic soln. 1.0 nM Cu^{2+}	0.89 nM ±0.02 (n=3)	%89.0
synthetic soln. 100 nM Cu^{2+}	96.36 nM ± 2.43 (n=3)	%96.4

e) Regeneration of Modified Electrode and Interferences Study

To eliminate the Cu^{2+} ions from the surface of the modified electrode, the electrode was immersed in 0.001 M EDTA solution with pH = 3.0 at potential +500 mV for 100 sec. The cleaned electrode was checked by DPV. The interference of other species for the reduction of Cu^{2+} on the modified gold electrode was investigated. The interfering effect was defined as a concentration of other species that can change the electrode response toward the analyte by more than 3 fold the standard deviation (3σ) on the analyte replicating measurement signals. The results indicated that Zn^{2+}, Cd^{2+}, Co^{2+}, Ni^{2+}, Fe^{2+}, and Ag^{+} ions concentration in 100 fold of the Cu^{2+} concentration showed no interference in the measurement. Although the peak current of Cu^{2+} was affected by 10 fold of Ca^{2+}, in the presence of 0.1 M KCl in Cu^{2+} solutions, Ca^{2+} does not interfere to 50 fold of Cu^{2+}. As explained in the text, the maximum accumulation of Cu^{2+} takes place at pH=6.5. Since K_{SP} of $Fe(OH)_3$ is about 6.3×10^{-38}, it can be concluded that the concentration of non precipitated free Fe^{3+} ions at this pH is about 1.992×10^{-15} M which does not interfere

with Cu^{2+} ions. By the way, the experimental results showed that 1000 fold of Fe^{3+} had no interfering effect on the response of the electrode toward Cu^{2+}. On the other hand, it is well known that interference of mercury (II) ions arises from deposition of Hg on the gold surface and altering Au-SAMs modified electrode to Hg-SAMs modified electrode. Therefore it should be considered that this type of SAMs modified electrodes is appropriate for Hg(II) ions free media.

Moreover, DPVs of the modified electrode after immersion in the copper free solution of each cation (5.0×10^{-4} M) at optimized conditions showed no cathodic current around +200 mV.

4. CONCLUSIONS

The new sensor was constructed based on a gold cysteamine self-assembled monolayer (SAM) electrode, functionalized with L-Lysine using the glutaraldehyde as a linker. The electrochemical studies revealed that a physically and chemically stable film of amino acid was formed. The amino and carboxylic functional groups on L-Lysine show great tendency for the accumulation of Cu^{2+}. The amino acid modified electrode exhibits high sensitivity to copper ions, which is attributed to the stable coordinate complex the peptide formed around the metal ion to give copper the preferred tetragonal coordination. The results show that tetragonal coordination complex of Cu^{2+} by nitrogen (N) and oxygen (O) provides high selectivity and sensitivity as well as 4N [14] or 4O [18] tetragonal coordination. The proposed electrode was compared with other chemically modified electrodes as Cu^{2+} sensor (Table 2). It is obvious that SAMs gold modified electrodes exhibit low detection limit and a wide linear range than the other types of modified electrodes. Among the amino acid SAMs modified electrodes, it has been proved that the steric repulsive force of end groups (NH_2, OH) as well as more bulky end groups (COOH, ferrocene) can reduce the surface coverage, packing density and ordering of the performed monolayer [20, 59]. By considering these properties, the L-Lysine SAMs modified electrode (this work) shows more packing order and a stable monolayer with higher sensitivity and selectivity, and a lower detection limit towards Cu^{2+}. In the case of the packing density of the monolayer, it is well known that layer by layer assembly followed by in situ functionalization of the monolayer is more favorable than the single layer assembly of synthesized thiol.

Table 2. Comparison of the present work with other chemically modified electrodes as Cu^{2+} sensor

No.	Electrode	Modifier	Electrochemical Method	Linear Range (M)	Detection Limit (M)	Interferences	Reference
1	ISE	electropolymerized polyindole	potentiometric	1.0×10^{-4}-1.0×10^{-3}	8×10^{-6}	Ni^{2+}, Co^{2+}, Fe^{2+} and Zn^{2+}	[49]
2	ISE	carboxylated thiacrown ether	potentiometric	1.0×10^{-7} - 1.0×10^{-3}	6.3×10^{-8}	Ag^{+}	[50]
3	carbon paste	Salen Schiff base	ASV	3.4×10^{-10}– 3.3×10^{-7}	1.8×10^{-10}	-	[51]
4	carbon paste	SAM of mercapto compounds on gold nanoparticles	potentiometric	7.9×10^{-9}– 3.2×10^{-2}	3.5×10^{-9}	-	[52]
5	conducting copolymer	iminodiacetatic acid (IDA)	SWV	1.0×10^{-7} – 1.0×10^{-5}	-	no interference by Ni^{2+}, Ca^{2+}, K^{+} and Pb^{2+}	[53]
6	Poly(3-thiopheneacetic acid)	Gly–Gly–His tripeptide	SWV	3.1×10^{-10}- 3.1×10^{-7}	-	-	[54]
7	Polypyrrole nanowire	Gly-Gly-His tripeptide	SWV	2.0×10^{-8}– 3.0×10^{-7}	-	no interference by Cr^{3+} and Ni^{2+}	[55]
8	gold	L-cysteine SAM	OSWV	1.3×10^{-9} - 1.6×10^{-7}	-	Ni^{2+}, Ag^{+}	[56]
9	gold	d,l-Penicillamine SAM	DPSV	3.1×10^{-9} – 7.9×10^{-7}	-	-	[57]
10	gold	thiodimethylglyoxime (TDMG) SAM	DPSV	4.7×10^{-9}- 4.7×10^{-7}	-	-	[57]

Table 2. (Continued)

11	gold	3-Mercaptopropionic and glutathione SAM	DPV	1.0×10^{-5}-1.0×10^{-4}	-	-	[58]
12	gold	cysteine SAM	DPV	8.0×10^{-10}-8.0×10^{-8}	3.9×10^{-10}	Ni^{2+}	[17]
13	gold	cysteamine SAM	EIS and OSWV	4.7×10^{-10}-5.0×10^{-6}	7.9×10^{-11}	-	[4a]
14	gold	2,3- dimercaptosuccinic acid SAM	DPV	4.7×10^{-8}-3.5×10^{-6}	2.0×10^{-8}	-	[24]
15	gold	cysteamine-glutaraldehyde-L-lysine SAM	DPV	1.0×10^{-12} - 1×10^{-6}	1.2×10^{-13}	Ca^{2+} interfere in phosphate buffer, but doesn't interfere in the presence of 0.1 M KCl	This Work

ASV=Anodic Stripping Voltammetry, SWSV=Square Wave Stripping Voltammetry, DPV=Differential Pulse Voltammetry, OSWV=Osteryoung Square Wave Voltammetry, DPSV=Differential Pulse Stripping Voltammetry, SWV=Square Wave Voltammetry, EIS=Electrochemical Impedance Spectroscopy, ISE=Ion Selective Electrode, SAM=Self Assembled Monolayer

In this work, the fabricated SAMs modified gold electrode was successfully tested for quantitative analysis of Cu^{2+} by differential pulse voltammetry (DPV). The DPV peak currents indicated a linear relationship with pCu in the range of 1.0×10^{-12} to 1.0×10^{-6} M, with a detection limit of 1.2×10^{-13} M. The sensor exhibited high selectivity for Cu^{2+}. As a benefit of *in-situ* functionalization of the monolayer surface, the analytical stability of the sensor was studied for a relatively long period of time.

Acknowledgments- The authors greatly appreciate the Firozabad Branch, and the Science and Research Branch of Islamic Azad University for providing facilities for this work.

REFERENCES

1. Ulman, A. (1996). Formation and structure of self-assembled monolayers. *Chem. Rev.*, *96*, 1533-1554.
2. Love, J. C., Estroff, L. A., Kriebel, J. K., Nuzzo, R. G. & Whitesides, G. M. (2005). Self-assembled monolayers of thiolates on metals as a form of nanotechnology. *Chem. Rev.*, *105*, 1103-1170.
3. Denayer, J., Delhalle, J. & Mekhalif, Z. (2009). Comparative study of copper surface treatment with self assembled monolayers of aliphatic thiol, dithiol and dithiocarboxylic acid. *J. Electroanal. Chem.*, *637*, 43-49.
4. (a) Shervedani, R. K. & Mozaffari, S. A. (2006). Copper(II) nanosensor based on a gold cysteamine self-assembled monolayer functionalized with salicylaldehyde. *Anal. Chem*., *78*, 4957-4963. (b) Mozaffari, S. A.; Chang, T. & Park, S. M. (2010).Self-assembled monolayer as a pre-concentrating receptor for selective serotonin sensing. *Biosens. Bioelectron*, *26,* 74-79.
5. Chow, E. & Gooding, J. J. (2006). Peptide modified electrodes as electrochemical metal ion sensors. *Electroanalysis*, *18*, 1437-1448.
6. Protsailo, L. V. & Fawcett, W. R. (2000). Studies of electron transfer through self-assembled monolayers using impedance spectroscopy. *Electrochim. Acta*, *45*, 3497-3505.
7. Laibinis, P. E. & Whitesides, G. M. (1992). Self-assembled monolayers of n-alkanethiolates on copper are barrier films that protect the metal against oxidation by air. *J. Am. Chem. Soc.*, *114*, 9022-9028.
8. Kitagawa, K.; Morita, T. & Kimura, S. (2005). Electron transfer in metal−molecule−metal Junction composed of self-assembled monolayers of helical peptides carrying redox-active ferrocene units. *Langmuir*, *21*, 10624-10631.
9. Chen, J., Rawlett, Z. M. A. & Tour, J. M. (1999). Large on-off ratios and negative differential resistance in a molecular electronic device. *Science*, *286*, 1550-1552.
10. Arya, S. K., Solanki, P. R.; Datta, M. & Malhotra, B. D. (2009). Recent advances in self-assembled monolayers based biomolecular electronic devices. *Biosens. Bioelectron.*, *24*, 2810-2817.

11. Forzani, E. S., Solis, V. M. & Calvo, E. J. (2000). Electrochemical behavior of polyphenol oxidase immobilized in self-assembled structures layer by layer with cationic polyallylamine. *Anal. Chem.*, *72*, 5300-5307.
12. Shervedani, R. K., Mehrjardi, A. H. & Zamiri, N. (2006). A novel method for glucose determination based on electrochemical impedance spectroscopy using glucose oxidase self-assembled biosensor. *Bioelectrochemistry*, *69*, 201-208.
13. Crisponi, G., Marina Nurchi, V.; Fanni, D.; Gerosa, C. & Nemolato, S. G. (2010). Copper-related diseases: from chemistry to molecular pathology. *Coordination Chem. Rev.*, *254*, 876-889.
14. Yang, W., Gooding, J. J. & Hibbert, D. J. B. (2001). Characterisation of gold electrodes modified with self-assembled monolayers of L-cysteine for the adsorptive stripping analysis of copper. *J. Electroanal. Chem.*, *516*, 10-16.
15. Berchmans, S., Arivukkodi, S. & Yegnaraman, V. (2000). Self-assembled monolayers of 2-mercaptobenzimidazole on gold: stripping voltammetric determination of Hg(II). *Electrochem. Commun.*, *2*, 226-229.
16. Shervedani, R. K. & Mozaffari, S. A. (2006). Impedimetric sensing of uranyl ion based on phosphate functionalized cysteamine self-assembled monolayers. *Anal. Chim. Acta*, *562*, 223-228.
17. Shervedani, R. K.; Bagherzadeh, M.; Sabzyan, H. & Safari, R. (2009). One-impedance for one-concentration impedimetry as an electrochemical method for determination of the trace zirconium ion. *J. Electroanal. Chem.*, *633*, 259-263.
18. Liu, A. C., Chen, D. C., Lin, C. C., Chou, H. H. & Chen, C. H. (1999). Application of cysteine monolayers for electrochemical determination of sub-ppb copper(II). *Anal. Chem., 71,* 1549.
19. Mandler, D. & Turyan, I. (1996). Applications of self-assembled monolayers in electroanalytical chemistry. *Electroanalysis*, *8*, 207-213.
20. Wink, Th.; van Zuilen, S. J.; Bult, A. & van Bennekom, W. P. (1997). Self-assembled monolayers for biosensors. *Analyst*, *122*, 43R-50R.
21. Mirsky, V. M. (2002). New electroanalytical applications of self-assembled monolayers. TrAC *Trends Anal. Chem.*, *21*, 439-450.
22. Postlethwaite, T. A., Hutchison, J. E., Hathcock, K. W. & Murray, R. W. (1995). Optical, electrochemical, and electrocatalytic properties of self-assembled thiol-derivatized porphyrins on transparent gold films. *Langmuir*, *11*, 4109-4116.
23. Rahman, M. A., Won, M. S. & Shim, Y. B. (2003). Characterization of an EDTA bonded conducting polymer modified electrode: its application for the simultaneous determination of heavy metal ions. *Anal. Chem.*, *75*, 1123-1129.
24. Mohadesi, A. & Taher, M. A. (2007). Voltammetric determination of Cu(II) in natural waters and human hair at a meso-2,3-dimercaptosuccinic acid self-assembled gold electrode. *Talanta*, *72*, 95-100.
25. Wang, F., Liu, Q., Wu, Y. & Ye, B. (2009). Langmuir–Blodgett film of *p-tert*-butylthiacalix[4]arene modified glassy carbon electrode as voltammetric sensor for the determination of Ag^{+}. *J. Electroanal. Chem.*, *630*, 49-54.
26. Park, J. Y., Lee, Y. S., Kim, B. H. & Park, S. M. (2008). Label-free detection of antibody−antigen interactions on (*R*)-lipo-diaza-18-crown-6 self-assembled monolayer modified gold electrodes. *Anal. Chem.*, *80*, 4986-4993.
27. Markovich, I. & Mandler, D. (2001). Disorganised self-assembled monolayers (SAMs): the incorporation of amphiphilic molecules. *Analyst*, *126*, 1850-1856.
28. Mozaffari, S. A., Chang, T. & Park, S. M. (2009). Diffusional electrochemistry of cytochrome *c* on mixed captopril/3-mercapto-1-propanol self-assembled monolayer modified gold electrodes. *J. Phys. Chem. C*, *113,* 12434-12442.
29. Shervedani, R. K. & Mozaffari, S. A. (2005). Preparation and electrochemical characterization of a new nanosensor based on self-assembled monolayer of cysteamine functionalized with phosphate groups. *Surf. Coat. Technol.*, *198,*123-128.

30. Rubinstein, I., Steinberg, S., Tor, Y., Shanzer, A. & Sagive, J. (1988). Ionic recognition and selective response in self-assembling monolayer membranes on electrodes. *Nature*, *332*, 426-429.
31. Steinberg, S., Tor, Y., Sabatani, E. & Rubinstein, I. (1991). Ion-selective monolayer membranes based upon self-assembling tetradentate ligand monolayers on gold electrodes. 2. Effect of applied potential on ion binding. *J. Am. Chem. Soc.*, 113, 5176-5182.
32. Steinberg, S. & Rubinstein, I. (1992). Ion-selective monolayer membranes based upon self-assembling tetradentate ligand monolayers on gold electrodes. 3. Application as selective ion sensors. *Langmuir*, *8*, 1183-1187.
33. Yang, N., Wang, X. & Wan, Q. (2006). Electrochemical reduction of Zn(II) ions on l-cysteine coated gold electrodes. *Electrochim. Acta*, *51*, 2050-2056.
34. Shervedani, R. K., Farahbakhsh, A. & Bagherzadeh, M. (2007). Functionalization of gold cysteamine self-assembled monolayer with ethylenediaminetetraacetic acid as a novel nanosensor. *Anal. Chim. Acta*, *587*, 254-262.
35. Turyan, I. & Mandler, D. (1994). Self-assembled monolayers in electroanalytical chemistry: Application of omega-mercaptocarboxylic acid monolayers for electrochemical determination of ultralow levels of cadmium(II). *Anal. Chem.*, *66*, 58-63.
36. Turyan, I. & Mandler, D. (1997). Selective Determination of Cr(VI) by a self-assembled monolayer-based electrode. *Anal. Chem*., *69*, 894-897.
37. Gooding, J. J., Hibbert, D. B. & Yang, W. (2001). Electrochemical metal ion sensors. exploiting amino acids and peptides as recognition elements. *Sensors*, *1*, 75-90.
38. Yang, W., Jaramillo, D., Gooding, J. J., Hibbert, D. B., Zhang, R., Willet, G. D. & Fisher, K. J. (2001). Sub-ppt detection limits for copper ions with Gly-Gly-His modified electrodes. *Chem. Commun*., *19*, 1982-1983.
39. Yang, W. R., Chow, E., Willett, G. D., Hibbert, D. B. & Gooding, J. J. (2003). Exploring the use of the tripeptide Gly-Gly-His as a selective recognition element for the fabrication of electrochemical copper sensors. *Analyst*, *128*, 712-718.
40. Chow, E., Hibbert, D. B. & Gooding, J. J. (2005). His-Ser-Gln-Lys-Val-Phe as a selective ligand for the voltammetric determination of Cd^{2+}. *Electrochem. Commun.*, *7*, 101-106.
41. Smalley, J. F., Chalfant, K., Feldberg, S. W., Nahir, T. M. & Bowden, E. F. (1999). An indirect laser-induced temperature jump determination of the surface pK_a of 11-mercaptoundecanoic acid monolayers self-assembled on gold. *J. Phys. Chem. B.*, *103*, 1676-1685.
42. (a) Jurczakowski, R., Hitz, C. & Lasia, A. (2004). Impedance of porous Au based electrodes. *J. Electroanal. Chem.*, *572*, 355-366. (b) Lasia, A. & Rami, A. (1990). Kinetics of hydrogen evolution on nickel electrodes. *J. Electroanal. Chem*., *294*, 123-141. (c) Boukamp, B. A. (1980). Package for impedance/admittance data analysis. *Solid State Ionics*, *18, 19*, 136-140. (d) Boukamp, B. A. (1986). Nonlinear least squares fit procedure for analysis of immittance data of electrochemical systems. *Solid State Ionics, 20*, 31-44.
43. Hoare, J. P. (1984). A cyclic voltammetric study of the gold-oxygen system. *J. Electrochem. Soc., 131*, 1808-1815. (b) Oesch, U. & Janata, J. (1983). Electrochemical study of gold electrodes with anodic oxide films formation and reduction behaviour of anodic oxides on gold. *Electrochim. Acta., 28*, 1237-1246.
44. (a) Macdonalds, R. (1987). *Impedance Spectroscopy*, 1st ed., New York, Wiley. b) Janek, R.P. & Fawcett, W. R. (1997). Impedance spectroscopy of self-assembled monolayers on Au(111): evidence for complex double-layer structure in aqueous $NaClO_4$ at the potential of zero charge. *J. Phys. Chem. B, 101*, 8550-8558.
45. Flink, S., Boukamp, B. A., van den Berg, A., van Veggel, F. C. J. M. & Reinhoudt, D. N. (1998). Electrochemical detection of electrochemically inactive cations by self-assembled monolayers of crown ethers. *J. Am. Chem. Soc*, *120*, 4652-4657.

46. Alfonta, L., Katz, E. & Willner, I. (2000). Sensing of acetylcholine by a tricomponent-enzyme layered electrode using faradaic impedance spectroscopy, cyclic voltammetry, and microgravimetric quartz crystal microbalance transduction methods. *Anal. Chem*, *72*, 927-935.
47. Xiao, Y., Ju, H.-X. & Chen, H. Y. (1999). Hydrogen peroxide sensor based on horseradish peroxidase-labeled Au colloids immobilized on gold electrode surface by cysteamine monolayer. *Anal. Chim. Acta., 391*, 73-82.
48. Jurczakowski, R.; Hitz, C. & Lasia, A. (2005). Impedance of porous gold electrodes in the presence of electroactive species. *J. Electroanal. Chem., 582*, 85-96.
49. Pandey, P. C. (1999). Copper (II) ion sensor based on electropolymerized undoped-polyindole modified electrode. *Sens. Actuators B, 54*, 210-214.
50. Wakida, S. I., Sato, N. & Saito, K. (2008). Copper(II)-selective electrodes based on a novel charged carrier and preliminary application of field-effect transistor type checker. *Sens. Actuators B, 130,* 187-192.
51. Ghiaci, M., Rezaei, B. & Arshadi, M. (2009). Characterization of modified carbon paste electrode by using Salen Schiff base ligand immobilized on SiO_2–Al_2O_3 as a highly sensitive sensor for anodic stripping voltammetric determination of copper(II). *Sens. Actuators B, 139,* 494-500.
52. Mashhadizadeh, M. H., Eskandari, Kh., Foroumadi, A. & Shafiee, A. (2008). Copper(II) modified carbon paste electrodes based on self-assembled mercaptocompounds-gold-nanoparticle. *Talanta 76,* 497-502.
53. Lina, M., Chob, M., Choea, W. S., Sonc, Y. & Lee, Y. (2009). Electrochemical detection of copper ion using a modified copolythiophene electrode. *Electrochimica Acta*, *54,* 7012-7017.
54. Lina, M., Chob, M. S., Choea, W. S. & Lee, Y. (2009). Electrochemical analysis of copper ion using a Gly-Gly–His tripeptide modified poly(3-thiopheneacetic acid) biosensor. *Biosens. Bioelectron.*, *25,* 28-33.
55. Lina, M., Choa, M., Choea, W. S., Yoob, J. B. & Lee, Y. (2010). Polypyrrole nanowire modified with Gly-Gly-His tripeptide for electrochemical detection of copper ion. *Biosens. Bioelectron.*, *26,* 940-945
56. Yang, W., Gooding, J. J. & Hibbert, D. B. (2001). Characterisation of gold electrodes modified with self-assembled monolayers of L-cysteine for the adsorptive stripping analysis of copper. *J. Electroanal. Chem., 516,* 10-16.
57. Profumo, A., Merli, D. & Pesavento, M. (2006). Self-assembled monolayer modified gold electrodes for traces Cu(II) determination. *Anal. Chim. Acta, 557*, 45-51.
58. Zeng, B., Ding, X. & Zhao, F. (2002). Voltammetric response of glutathione and 3-mercaptopropionic acid self-assembled monolayer modified gold electrodes to Cu(II). *Electroanalysis, 14*, 651.
59. Shervedani, R. K. & Hatefi-Mehrjardi, A. (2009). Comparative electrochemical behavior of glucose oxidase covalenty immobilized on mono-, di- and tetra-carboxylic acid functional Au-thiol SAMs via anhydride-derivatization route. *Sens. Actuators B, 137*, 195.